




Quantitative Structure-Activity Relationships of xanthen-3-one and xanthen-1,8-dione derivatives and design of new compounds with enhanced antiproliferative activity on HeLa cervical cancer cells

Selma Zukić, Slavica Oljatic, Katarina Nikolic, Elma Veljović, Selma Špirtović-Halilović, Amar Osmanović & Davorka Završnik

To cite this article: Selma Zukić, Slavica Oljatic, Katarina Nikolic, Elma Veljović, Selma Špirtović-Halilović, Amar Osmanović & Davorka Završnik (2020): Quantitative Structure-Activity Relationships of xanthen-3-one and xanthen-1,8-dione derivatives and design of new compounds with enhanced antiproliferative activity on HeLa cervical cancer cells, Journal of Biomolecular Structure and Dynamics, DOI: [10.1080/07391102.2020.1775125](https://doi.org/10.1080/07391102.2020.1775125)

To link to this article: <https://doi.org/10.1080/07391102.2020.1775125>

 View supplementary material 

 Accepted author version posted online: 28 May 2020.

 Submit your article to this journal 

 Article views: 11

 View related articles 

 View Crossmark data 

Quantitative Structure-Activity Relationships of xanthen-3-one and xanthen-1,8-dione derivatives and design of new compounds with enhanced antiproliferative activity on HeLa cervical cancer cells

Selma Zukić^a, Slavica Oljacić^{b*}, Katarina Nikolić^b, Elma Veljović^a, Selma Špirtović-Halilović^a, Amar Osmanović^a, Davorka Završnik^a

^aFaculty of Pharmacy, Department of Pharmaceutical Chemistry, University of Sarajevo, Zmaja od Bosne 8, 71 000 Sarajevo, Bosnia and Herzegovina

^bFaculty of Pharmacy, Department of Pharmaceutical Chemistry, University of Belgrade, Vojvode Stepe 450, 11000 Belgrade, Serbia

*Corresponding author: Slavica Oljacić, Department of Pharmaceutical Chemistry, Faculty of Pharmacy, University of Belgrade, Vojvode Stepe 450, 11000 Belgrade, Serbia. Email: slavica.oljacic@pharmacy.bg.ac.rs

Abstract

Xanthen derivatives have become a group of molecules of great importance in discovering of new anticancer drugs. Recent studies of our group performed on xanthen-3-one and xanthen-1,8-dione derivatives have shown their antiproliferative activity on HeLa cervical cell lines. Obtained IC₅₀ values together with calculated molecular descriptors were subjected to Quantitative Structure-Activity Relationship (QSAR) study in order to identify the most

relevant molecular features responsible for the observed antiproliferative activity of compounds. Partial Least Square statistical method and the same training and test set were used to obtain statistical parameters for internal and external validation in 2D- and 3D- QSAR study. The obtained QSAR models have shown next results: 2D-QSAR: $R^2=0.741$, $Q^2=0.792$, $R^2_{\text{pred}}=0.875$ and 3D-QSAR: $R^2=0.83$, $Q^2=0.951$, $R^2_{\text{pred}}=0.769$. Based on the performed QSAR analysis and calculated ADMET properties, novel xanthene derivatives with enhanced antiproliferative activity were designed.

Keywords: xanthene, HeLa, antiproliferative activity, QSAR, ADMET

Abbreviations:

2D, 3D, Two, three dimensional; **ADMET**, Absorption, distribution, metabolism, excretion, toxicity; **BJ**, Human fibroblast; **DMEM**, Dulbecco's modified Eagle medium; **DMSO**, Dimethyl sulfoxide; **FBS**, Fetal bovine serum; **FFD**, Fractional factorial design; **HeLa**, Cervical cancer cell; **HOMO**, Highest Occupied Molecular Orbital; **IC₅₀**, The concentration that causes a 50% reduction of the cell growth; **LOO**, Leave one out; **LUMO**, Lowest Unoccupied Molecular Orbital; **LV**, Latent variables; **MTT**, 3-(4,5-dimethylthiazole-2-yl)-2,5-diphenyl tetrazolium bromide; **PBS**, Phosphate Buffered Saline; **PG**, Percentage of growth; **PLS**, Partial Least Square; **PM3**, Parameterized Model number 3; **PRESS**, Prediction Sum of Squares; **RMSEE**, Root mean squared error of estimation; **RMSEP**, Root mean squared error of prediction; **SIMCA**, Soft Independent Modeling of Class Analogy; **VIP**, Variable importance in the projection; **QSAR**, Quantitative Structure-Activity Relationship.

1. Introduction

Xanthene derivatives are of great importance in the process of discovering new drugs. The biological activity of this group of compounds is related to their tricyclic structure and depends on the type and position of various substituents (Pinto et al., 2005). Therefore xanthene is an attractive scaffold for design and synthesis of novel pharmacological agents such as metabotropic glutamate antagonist (Ornstein et al., 1998), trypanothione reductase (TryR) inhibitors (Chibale et al., 2003), chloroquine (CQ) potentiating agents (Chibale et al., 2003), chemokine receptor (CCR1) antagonists (Naya et al., 2001). Some of the biological activities that xanthene derivatives possess are anticancer (Castanheiro et al., 2009; Giri et al., 2010; Pedro et al., 2002; Wang et al., 2018), antioxidant (Santos et al., 2010), antimicrobial (Omolo et al., 2011), cardioprotective (Jiang et al., 2004), anti-inflammatory (Yen et al., 2012), antimalarial (Winter et al., 1997), and as inhibitors of some enzymes such as topoisomerase (Woo et al., 2007), aromatase (Recanatini et al., 2001), and α -glucosidase (Santos et al., 2018). Several review articles detail the numerous biological activities of xanthene derivatives, including the inhibitory activities of a number of enzymes (Ahmad, 2016; Kumar et al., 2017; Na, 2009; Pinto et al., 2005; Santos et al., 2018).

The anticancer activity has been observed in many natural products such as gambogic acid, α -mangostin, and psorospermin and is related to the xanthene nucleus and its ability to inhibit the enzyme topoisomerase II (Na, 2009). Promising cytotoxicity on HeLa tumor cell lines has been shown as well on a series of synthesized substituted xanthene derivatives (Giri et al., 2010; Woo et al., 2007). In our previous studies performed on xanthen-3-one and xanthene-1,8-dione, antiproliferative activity on HeLa cervical carcinoma cell lines has been in the range from 0.7 μ M to 100 μ M. It has been found that two most potent compounds from these series are

xanthen-3-one derivative with CF_3 substituent in C-4' position of the phenyl ring and IC_{50} value $0.7 \mu\text{M}$ (Veljović et al., 2019), and xanthen-1,8-dione with bromine in C-2' and methyl group in C-4' of the phenyl ring with IC_{50} value $5.6 \mu\text{M}$ (Zukić et al., 2018).

A literature survey has revealed several reports relating to Quantitative Structure-Activity Relationship (QSAR) studies of xanthone derivatives. In these studies, the Multiple Linear Regression (MLR) method was applied to establish the relationship between molecular descriptors on the one side and biological activity on the other (Alam & Khan, 2014; Liu et al., 2008; Núñez et al., 2004). According to the created QSAR models, H-bonding substituents, softness, and the number of aromatic rings can be utilized to model the inhibitory activity toward α -glucosidase (Liu et al., 2008). Descriptors like the E-state index, molecular connectivity and shape descriptors are important for MAO inhibitory activity of xanthenes derivatives (Núñez et al., 2004) while dielectric energy, group count (hydroxyl), the logarithm of the partition coefficient between n-octanol and water, shape index basic (order 3), and the solvent-accessible surface area are descriptors with significant influence on anticancer activity against HeLa cell lines (Alam & Khan, 2014).

To the best of our knowledge, none of the articles so far reported is deal with QSAR study of xanthen-3-one and xanthen-1,8-dione derivatives. The main objective of this study is to determine the antiproliferative activity of 8 new xanthen-3-one derivatives on HeLa cervical cancer cell lines and to use them together with previously published IC_{50} values for 2D- and 3D-QSAR analysis. QSAR models created by Partial Least Square (PLS) regression will be used for identification of the most important structural determinants responsible for the antiproliferative activity of examined compounds and for the design of new drugs with enhanced antiproliferative activity.

2. Materials and methods

2.1. Molecular set and antiproliferative evaluation of xanthene derivatives

All of the examined xanthene derivatives which can be divided into two series: series I (9-aryl substituted 2,6,7-trihydroxyxanthen-3-one) presented in Table 1 and series II (3,3,6,6,-tetramethyl-9-aryl-substituted-xanthen-1,8(2H)-dione) presented in Table 2 were previously synthesized at the Laboratory of our Department of Pharmaceutical Chemistry and published (Applova et al., 2018; Veljović et al, 2017; Veljović et al, 2019; Veljović et al, 2018; Veljović et al, 2015; Zukić et al., 2018).

Most of the antiproliferative activity of 9-aryl substituted 2,6,7-trihydroxyxanthen-3-ones and 3,3,6,6,-tetramethyl-9-aryl-substituted-xanthen-1,8(2H)-diones on HeLa cancer cell lines have been determined in our previous studies (Applova et al., 2018; Veljović et al, 2017; Veljović et al, 2019; Veljović et al, 2018; Veljović et al, 2015; Zukić et al., 2018). In this work, antiproliferative activity on HeLa cervical cancer cells will be determined for 8 new xanthen-3-one derivatives (compounds **13-20**, Table 1.).

2.1.1 Cell culturing

The cell lines HeLa (cervical carcinoma) and BJ (Human fibroblast), were cultured as monolayers and maintained in Dulbecco's modified Eagle medium (DMEM, Lonza, Austria) supplemented with 10 % fetal bovine serum (FBS), 2 mM *L*-glutamine, 100 U mL⁻¹ penicillin and 100 µg mL⁻¹ streptomycin in a humidified atmosphere with 5 % CO₂ at 37 °C. The cells were maintained in culture until 80 % of confluence and at that point washed by PBS (Phosphate Buffered Saline, GIBCO, USA) and detached from the surface by use of 0.25 % trypsin solution (LONZA, Basel, Switzerland). Trypan blue solution was used to determine cell

viability during regular passaging on an automatic cell counter (Countess, Invitrogen, USA). Morphology was determined under the light microscope (Axio Vision-Zeiss, Germany).

2.1.2 Proliferation assays

A panel of adherent tumor cell lines was inoculated onto a series of standard 96-well microtiter plates on day 0, at 5000 cells per well. Test agents were then added in five, 10-fold dilutions (0.01 to 100 μ M) and incubated for 72 h. Working dilutions were freshly prepared in the growth medium on the day of testing. The solvent (DMSO) was also tested for eventual inhibitory activity by adjusting its concentration to be the same as in the working solutions (DMSO concentration never exceeded 0.1 %). After 72 h of incubation, the cell growth rate was evaluated by performing the MTT assay. End-point absorbance was measured at 570 nm. Each test point was performed in quadruplicate in three individual experiments. Experimentally determined absorbance values were transformed into a cell percentage growth (PG) using the formulas proposed by NIH and described previously (Gazivoda et al., 2008). This method directly relies on control cells on the day of the assay because it compares the growth of treated cells with the growth of untreated cells in control wells on the same plate. The results are therefore a percentile difference from the calculated expected value. The IC₅₀ and LC₅₀ values for each compound were calculated from dose-response curves using linear regression analysis by fitting the mean test concentrations that give PG values above and below the reference value. If, however, all of the tested concentrations produce PGs exceeding the respective reference level of effect (*e.g.*, PG value of 50) for a given cell line, the highest tested concentration is assigned as the default value (in the screening data report that default value is preceded by a ">" sign).

For the evaluation of cell proliferation, the cells were treated with compounds at concentrations of 0.01 μ M to 100 μ M for 72 h. MTT assay was used to assess the antiproliferative activity of the synthesized compounds with their activity expressed as IC₅₀.

2.2 QSAR studies of xanthen-3-one and xanthen-1,8-dione derivatives

2.2.1 Selection of the training and test set compounds

From the initial molecular data set of 45 compounds only 27 active compounds ($pIC_{50} > 4$) of 9-aryl substituted 2,6,7-trihydroxyxanthen-3-one and 3,3,6,6-tetramethyl-9-aryl-substituted-xanthen-1,8(2H)-dione were used for QSAR study (Tables 1 and 2). Compounds were divided into the training set (N=18): 1, 3, 4, 7, 8, 9, 10, 11, 13, 14, 16, 18, 20, 4-II, 16-II, 18-II, 20-II, 22-II and test set (N=9): 2, 6, 12, 15, 17, 19, 3-II, 14-II, 24-II by random selection taking into account that whole range of experimental pIC_{50} values is homogeneously distributed in both training and test set.

Although xanthene derivatives are structurally similar, the applicability domain was also set by analyzing minimum and maximum values of the descriptors of the test set against the minimum and maximum values of the descriptors of the training set. Molecules from the test set with descriptors values close to the upper limits for more than 3 descriptors of the training set were excluded, such as with compound 14-II.

2.2.2 Geometry optimization

ChemDraw 7.0.1 program (Cambridge Soft Corporation, 2002) was used to build the atomic coordinates of the examined compounds in which dominant microspecies at pH 7.4 were further selected using Marvin Sketch 6.1.0 software (Chem Axon, 2017). At the initial step of geometry optimization semi-empirical/PM3 (Parameterized Model number 3) method (Stewart, 1989a; Stewart, 1989b), followed by *ab initio* Hartree Fock/3-21G method (Roothaan, 1951) using Gaussian09 software (Frisch et al., 2009) included in ChemBio3D Ultra 13.0 (Cambridge Soft Corporation, 2015) program was applied.

2.2.3 Calculation of molecular descriptors

For all optimized molecular structures molecular descriptors were calculated using Dragon 6 (Talete srl, 2010; Todeschini & Consonni, 2009), ChemBio3D Ultra 13.0 (Cambridge Soft Corporation, 2015), and Gaussian09 software (Frisch et al., 2009). In addition, quantum chemical descriptors such as chemical potential (μ), electronegativity (χ), chemical hardness (η), and chemical softness (S) (Thanikaivelan et al., 2000) obtained from HOMO (Highest Occupied Molecular Orbital) and LUMO (Lowest Unoccupied Molecular Orbital) energy calculated by Density Functionals Theory using the B3LYP exchange-correlation hybrid functional and 6-31+G* basis sets (Frisch et al., 2009) were added to the initial set of molecular descriptors. Descriptors with intercorrelation lower than 0.90 were used for QSAR analysis. In the end, approximately 400 descriptors were applied to obtain a 2D-QSAR model.

2.2.4 Development of QSAR models

The quantitative regression analysis was performed to investigate the correlations between antiproliferative activity as a dependant variable (expressed as the negative logarithm of IC_{50} values, pIC_{50}) and calculated molecular descriptors as an independent variable. The 2D-QSAR model was created using PLS (Partial Least Square) regression (Wold et al., 2001) as a statistical method incorporated in the SIMCA (Soft Independent Modeling of Class Analogy) 14.1 software (Umetrics AB, 2015). The PLS method was chosen because of the possibility of analyzing a large number of descriptors as independent variable X against the number of compounds tested as dependent variable Y (Cramer 1993).

Variable importance in the projection (VIP) is used for the selection of molecular descriptors. VIP represents the influence of each x variable (x_k) on Y and X matrices and it is calculated for each variable. Every time one variable was excluded from the matrix and model was created again with new R^2 , $Q^2(Y)$, RMSEE, F ratio, p-value parameters (Gagić et al., 2016).

The 3D-QSAR model was created using the same training and test set used to develop the 2D-QSAR model. The 3D-QSAR study was performed by calculating steric and electrostatic 3D interaction energies between compounds and chemical probe: DRY (hydrophobic interactions), O (carbonyl oxygen, H-bond donor), N1(H-bond acceptor) and TIP (shape of molecule). Partial Least Square regression analysis was performed with Pentacle software using GRID independent variables (GRIND and GRIND2) as molecular descriptors and antiproliferative activity as dependent variables (Cramer et al., 1988; Molecular Discovery Ltd, 2009). The selection of the most important variables from the initial number was performed with fractional factorial design (FFD) (Baroni et al., 1993). Regression analysis was repeated and the new model with R^2 and Q^2 statistical parameters was obtained. The initial set of variables was reduced to 144. The number of the latent variable (LV) was set up to 5. After PLS analysis an optimal number of latent variables was selected based on the statistical results.

2.2.5 Internal and external validation of the models

Internal validation of the models was performed by leave-one-out (LOO) cross-validation. After excluding all compounds ones, the squared sum of differences between experimental and Leave One Out Y predicted values $e(i)$ for all created models was calculated by equation (1).

$$PRESS = \sum_{i=1}^n e_{(i)}^2 \quad (1)$$

Obtained predictive residual sum of squares (PRESS) was used for calculation of corresponding cross-validated squared correlation coefficient (Q^2) according to equation (2):

$$Q^2 = 1 - \frac{PRESS}{\sum(Y_{obs(training)} - \bar{Y}_{training})^2} \quad (2)$$

In order to obtain a model with good predictive capability value of Q^2 should be greater than 0.5 (Golbraikh & Tropsha, 2002).

In addition, statistical parameters such as R^2 (square of the correlation coefficient), the F ratio, the p-value, and RMSEE (root mean squared error of estimation) (Eq.3) were applied for the estimation of robustness and predictive ability of the models.

$$RMSEE = \sqrt{\frac{PRESS}{n-2}} \quad (3)$$

Robustness of the QSAR models, as well as an overfitting due to the chance correlation, were also assessed by the response permutation test (Y scrambling). Y variable was randomly shuffled and a new QSAR model was built using the independent variables. This procedure was repeated 100 times and the new PLS model was built. The intercepts of these regression lines should not be higher than 0.3–0.4 for R^2 intercept and 0.05 for Q^2 intercept (Wold et al., 1995).

Besides, the quality and predictive power of created models were estimated by external validation using parameters such as RMSEP (root mean squared error of prediction) in Eq. (4), R^2_{pred} in Eq. (5) (Tropsha, 2010) and r^2_m metrics in Eqs (6 and 7):

$$RMSEP = \sqrt{\frac{PRESS}{n}} \quad (4)$$

$$R^2_{pred} = 1 - \frac{\sum(Y_{obs}(test) - \bar{Y}_{pred}(test))^2}{\sum(Y_{obs}(test) - \bar{Y}_{training})^2} \quad (5)$$

$$r^2_m = r^2 \left(1 - \sqrt{|r^2 - r_0^2|} \right) \quad (6)$$

$$r_m^{/2} = \left(1 - \sqrt{|r^2 - r_0^{/2}|} \right) \quad (7)$$

For good predictive properties of the QSAR model, values of the r^2_m and $r_m^{/2}$ should be close and higher than 0.5. Average values \bar{r}_m^2 of r^2_m and $r_m^{/2}$ should be > 0.5 . The difference or delta r^2_m (Δr^2_m) between them is expected to be lower than 0.2 while R^2_{pred} should be higher than 0.5 (Ojha et al., 2011; Software Tools, n.d.).

3. Results and discussion

In this paper, anticancer activity of eight 9-aryl substituted 2,6,7-trihydroxyxanthen-3-ones is reported. The antiproliferative activity of all given compounds was tested against HeLa (cervical carcinoma) cell lines and BJ (Human fibroblast) as normal (non-tumor) cells. Compounds concentrations required to inhibit tumor cell proliferation by 50 % (IC_{50} values) are presented in Table 3.

According to obtain IC_{50} values, the strongest activity showed compound **14** with chlorine atom in *para* position on the phenyl ring. Introduction of halogen substituents in *para* position is important for antiproliferative activity, while substituents in other position decrease activity, which correlate well with already published study (Veljović et al., 2019). The weakest antiproliferative activity showed compound **18** with a hydroxyl group in position C-2 and NO_2 group in position C-5 on the phenyl ring. Biological comparative effects, as a function of the nature of the substituents, reveals that the insertion of the chlorine atom in *para* position on the aryl ring of the xanthen derivatives increases their antiproliferative activity.

All these findings together with activities presented in Tables 1 and 2 clearly suggest better activity of 9-aryl substituted 2,6,7-trihydroxyxanthen-3-one compared to 9-aryl substituted xanthen-1,8(2H)-dione, among which majority of the tested compounds exerted antiproliferative effects at a concentration higher than 100 μ M or at a slightly lower level.

3.1 QSAR study

Data set of 26 molecules consisting of 19 compounds belonging to 9-aryl substituted 2,6,7-trihydroxyxanthen-3-one and 7 compounds belonging to 9-aryl-substituted xanthen-1,8(2H)-dione was subjected to QSAR analysis (Table 1 and 2). The selected data set covered a wide range of biological activity with pIC_{50} values from 4.008 to 6.154 (Tables 1 and 2). For both, 2D- and 3D-QSAR study the same training set consisting of 18 compounds and a test set consisting

of 8 compounds were used. By applying comprehensive internal and external validation optimal 2D- and 3D-QSAR models were selected and discussed while the predicted activities and ADMET characteristics of the designed compounds indicated on the great importance and quality of the performed QSAR study.

3.1.1 2D-QSAR study

In the course of 2D-QSAR model building, descriptors with the lowest VIP values were successively removed from the model. For each new PLS model statistical parameters of internal (R^2 , Q^2 , RMSEE, F, p), and external validation (RMSEP, R^2_{pred}) were calculated and compared with the statistical data obtained in the previous model. As the results, 2D-QSAR model with four descriptors were selected based on VIP scores and achieved statistical requirements. The statistical parameters of internal and external validation are presented in Table 4.

High values of Q^2 and R^2 (Q^2 :0.741, R^2 :0.792) and low values of RMSEE and RMSEP (RMSEE:0.289, RMSEP:0.152) indicated on the high prognostic capacity of the created model. A Scatter plot of observed vs predicted activities is presented in *Fig. 1*.

For further improvement of external validation, r^2m matrices were applied. Obtained parameters (R^2_{pred} :0,875, rm^2 :0,89, reverse rm^2 :0,93, average rm^2 : 0,91, delta rm^2 : 0,03) confirmed that model is predictive and robust while Y-scrambling test with obtained intercept values of the R^2 (0.0, 0,0836) and Q^2 (0.0, -0,322)) confirmed that model was not obtained by chance (*Fig. S1*).

Four selected descriptors such as GATS3s, GATS3i, clogP, P_VSA_LogP_5 have shown the highest influence on antiproliferative activity of xanthene derivatives and their VIP values are presented on (*Fig. S2*).

The influence of these descriptors on the antiproliferative activity of xanthene derivatives depends on coefficient plots, where GATS3i, GATS3s have a negative influence, while clogP and P_VSA_LogP_5 have a positive influence on antiproliferative activity (*Fig.2*). Values of

the most important molecular descriptors in the 2D-QSAR model, their intercorrelation, and values of PLS coefficients are presented in Tables S1, S3, and S4, respectively (Supplementary Material).

GATS3i (Geary autocorrelation of lag 3 weighted by Ionization potential) (Talete srl, 2010) and GATS3s (Geary autocorrelation of lag 3 weighted by I-state) (Talete srl, 2010) represent 2D-Autocorrelation descriptors. This group of descriptors belongs to Geary autocorrelation of topological structures and describes the topology of the molecules or some of their parts depends on physicochemical properties with the weighting component embedded into descriptors (Sharma et al., 2010). According to the VIP scores and coefficient plots, GATS3i and GATS3s descriptors have the highest influence and are in a negative correlation with antiproliferative activity. It means that more active compounds will possess lower values of these descriptors. The most active compounds (**9**, **14**) possess substituents on the phenyl ring with lower ionization potential and have lower values of these descriptors, compared to the less active compounds which possess the higher values of these descriptors.

Partition coefficient octanol/water, clogP (Cambridge Soft Corporation, 2015) has shown a positive influence on antiproliferative activity (*Fig 2*). The most active compounds **9** and **11** have high values of this descriptor. The introduction of more lipophilic substituent could further increase antiproliferative activity.

P_VSA_LogP_5 represents Property labeled Van der Waals Surface Area (P_VSA) descriptors (Talete srl, 2010). This descriptor represents the sum of van der Waals surface area (VSA) over all atoms in a molecule with Ghose-Crippen log P (o/w) contribution in the range of (0;0.25) (Labute 2000). The molecule with the highest value of this descriptor is the most active compound **9** with trifluoromethyl group in C'-4 on the phenyl ring. According to the coefficient plot of the most important descriptors, the P_VSA_LogP_5 descriptor has a positive influence on antiproliferative activity. The conclusion is connected with the appearance of halogen

atoms, which shows that the presence of halogens is important for the antiproliferative activity of xanthene derivatives. Active compound **11** has also halogen element in its structure, with atom Br in C'-3 position which contributes also to higher Van der Waals Surface Area. The activity of the compound may be increased by introducing an additional number of halogen atoms, especially in position C'-4 on the phenyl ring. The logarithm of the partition coefficient between n-octanol and water and the solvent-accessible surface area also appeared as important descriptors in the QSAR study performed by Alam and Khan (2014).

Molecules **18** and **4-II** are compounds with low antiproliferative activities and low values of partition coefficient octanol/water and P_VSA_LogP_5. Both molecules possess OH group in C'-2 position while compound **18** has NO₂ group in C'-5 position of the phenyl ring and molecule **4-II** has OCH₃ group in C'-3 position of the phenyl ring. According to the coefficient plots of these descriptors, the introduction of lipophilic substituents may lead to increased antiproliferative activity. Molecules **18** and **4-II** have also shown higher values of most important descriptor GATS3i which means that antiproliferative activity may increase by adding halogen elements with lower ionization potential and removing functional groups with oxygen, such as OH and OCH₃. These substitutions may also increase the lipophilicity of the molecules.

3.1.2 3D-QSAR study

The most significant GRIND variables in the 3D-QSAR model were selected by using the FFD method and the optimal model was composed of three components (latent variables), LV=3. Obtained statistical results are presented in Table 4. High power of the created model to predict the activity of examined compounds in the training set was confirmed by the values $Q^2=0.83$, $R^2= 0.95$ and $RMSEE=0.147$ while its ability to reliably predict the activity of new compounds was proved by external validation ($RMSEP=0.207$, $R^2_{pred}=0.769$, rm^2 , reverse rm^2 , and average rm^2 are greater than 0.5 and Δrm^2 is lower than 0.2).

Compared to the results obtained by the 2D-QSAR model (Q^2 :0.741, R^2 : 0.792), the 3D-QSAR model can be used as more reliable for the prediction of the antiproliferative activity of newly designed compounds.

A Scatter plot of observed vs predicted activities of 3D-QSAR is presented in *Fig. 3*

Correlogram of 3D-QSAR study (*Fig. 4*) has shown that the most important variables with a positive influence on antiproliferative activity are v177 (TIP-TIP), v144 (TIP-TIP), v158 (TIP-TIP), and v395 (O-TIP), while the most important variables with negative influence on antiproliferative activity are v285 (DRY-TIP), v362(O-N1), v133(N1-N1), v25 (DRY-DRY), v212 (DRY-O), and v239 (DRY-N1), (*Table 5.*). PLS coefficients of selected variables are presented in Table S5 while intercorrelation matrix of descriptors is shown in Table S6 (Supplementary material).

Steric hot spots regions TIP-TIP v177, v144, v158 as favorable variables were detected in most active compounds **9**, **11**, **14** Favorable v144: TIP-TIP variable is not present only in the least active compound 4-II (*Fig. 5*). Favorable v158: TIP-TIP variable is present in all examined compounds while favorable v177: TIP-TIP variable is not present in compounds **1**, **3**, **13**, **16**, and **18**, mostly less active compounds. These variables which describe the distance between two steric hot spots have shown the importance of the C'-4 position of the phenyl ring. These sites are related to the presence of groups containing halogen elements in position C'-4 such as CF₃ in most active compound **9** and bromine in position C'-3 in also active compound **11**. Antiproliferative activity of the xanthene derivatives could be increased by introducing more voluminous group into para or meta position of the phenyl ring as well as in the xanthen nucleus.

Unfavorable v25: DRY-DRY variable is present mostly in less active compounds, while in compounds **3**, **4**, **9**, **11**, **13**, and **14** is not presented. Represent distance between two hydrophobic regions such as distance between the xanthene nucleus and NO₂ functional group in position C'-5

on phenyl ring (compound **18**) or distance within the xanthene nucleus (**4-II**). The presence of the NO₂ group at the distance of 10.0-10.4 Å from the xanthene nucleus is not favorable for antiproliferative activity.

Unfavorable v239: DRY-N1 variable is present in a majority of the examined compounds indicating that presence of the H-bond acceptor group in the xanthene nucleus at the distance 3.6-4 Å from the hydrophobic region of the phenyl ring is not favorable for activity.

Unfavorable v285: DRY-TIP variable is not present among the most active compounds (**8**, **9**, **11**, **14**). In less active compounds it is the distance between hydrophobic region and NO₂ group (**18**, **20**) or Br atom on the phenyl ring (**16-II**). Structural modification of phenyl ring could lead to increase activity.

Unfavorable v133: N1-N1 variable is present only in poor active compounds **10** and **20** and is formed between two H bond acceptors such as carbonyl oxygen in xanthene nucleus and NHCOCH₃ or NO₂ group in C'-4position of the phenyl ring at the distance 16.4-16.8 Å. The position of these substituents at the distance 16-16.4 Å from OH group in the xanthene nucleus is also unfavorable for antiproliferative activity (v362: O-N1).

Presence of hydrophobic region in the xanthene nucleus and OH group as an H-bond donor in C-7 position of the xanthene ring at the distance 11.2 -11.6 Å decrease antiproliferative activity (v212: DRY-O). Therefore the elimination of the C7-OH group could lead to increase activity.

According to the created 3D-QSAR model presence of a steric hot spot and hydrogen bond donor group at a certain distance is important for antiproliferative activity (v395:O-TIP). Those groups can be found within the xanthene nucleus or it is the distance between groups in the phenyl ring and xanthene nucleus.

Results of experimental and predicted values with residues of 2D- and 3D-QSAR studies are presented in Table S2 in Supplementary Material.

3.1.3. Design of new xanthene derivatives

In this work, 10 new xanthene derivatives were designed using created QSAR models (Fig. 6). Favorable variables TIP-TIP (v177, v144, v158) have shown the significance of steric regions in C'-4 position of the phenyl ring. Introducing methoxy and ethoxy groups as voluminous functional groups in the *para* position of the phenyl ring, such as in designed molecules **f**, **g** and **i** leads to higher antiproliferative activity. In addition, the introduction of halogen elements with lower ionization potential and higher lipophilicity, such as in the designed compounds **a**, **c**, and **d**, leads to increased antiproliferative activity. This is also in accordance with the results of the 2D-QSAR study indicating that increased lipophilicity of molecules could increase antiproliferative activity.

According to the unfavorable variable v212 (DRY-O) distance between the hydrophobic region of the xanthene nucleus and OH group in position C-7 of the xanthene nucleus has a negative influence on antiproliferative activity. Removing H bond donor OH group from position C-7 of the xanthene ring could increase antiproliferative activity. These modifications according to the negative variable v212 (DRY-O) are presented in all designed molecules.

The activity range of the experimental values of the initial data set was 4.008-6.154. According to the results of 3D-QSAR study and novel designed molecules, predicted values are higher and between 6.137-6.525 pIC₅₀. ADMET properties of the initial set of molecular structures (Table 6), as well as new designed xanthene derivatives, were calculated using ADMET Predictor software (Simulations Plus, 2013) and used for the final selection of the best drug candidates.

Predicted pIC₅₀ values (Table 7) of new designed xanthene derivatives have shown promising results and can be considered as good candidates for synthesis and experimental evaluation. According to the ADMET properties of the molecular data set used for the building of QSAR models, compound **16-II** violated two Lipinski's rules, molecular weight, and MlogP. All other compounds, as well as designed molecules, are in accordance with the Lipinski's rule. In

addition, all design compounds have low CYP risk and acceptable ADMET and TOX risk (Table 7).

Based on the predictive activity of new designed compounds and ADMET properties, molecular structures **b**, **g**, **h**, and **i** which possess low values of ADMET, CYP, and TOX risks and have not affinity to the hERG potassium channel in human, represent best drug candidates for the synthesis and further evaluation of cervical cancer treatment.

4. Conclusion

In this work, 2D- and 3D-QSAR studies were obtained using Partial Least Square regression analysis to predict the correlation between molecular descriptors as independent variables and antiproliferative activity as dependent variables. The most significant 2D descriptors that increase antiproliferative activity are clogP and P_VSA_LogP_5, while the most significant 3D descriptors that increase antiproliferative activity are v177 (TIP-TIP), v144 (TIP-TIP), v158 (TIP-TIP) and v395 (O-TIP). The 3D-QSAR study has shown better statistical parameters and was applied for the design of novel xanthene derivatives with enhanced antiproliferative activity on HeLa cervical cancer cells. Novel molecular structures were designed using 3D-QSAR most important variables and calculated ADMET properties. In conclusion, molecular structures **b**, **g**, **h**, and **i** are selected as the best drug candidates for the synthesis and further examination.

Acknowledgment

This work was supported by the Ministry of Education and Science of the Republic of Serbia, under Grant number 172033.

Disclosure statement

The authors have declared no conflict of interest.

The authors confirm that the data supporting the findings of this study are available within the article and its supplementary materials.

References

- Ahmad, I. (2016). Recent insight into the biological activities of synthetic xanthone derivatives. *European journal of medicinal chemistry*, 116, 267-280. DOI: 10.1016/j.ejmech.2016.03.058
- Alam, S., & Khan, F. (2014). QSAR and docking studies on xanthone derivatives for anticancer activity targeting DNA topoisomerase II α . *Drug design, development and therapy*, 8, 183. DOI: 10.2147/DDDT.S51577
- Applova, L., Veljović, E., Muratović, S., Karlickova, J., Macakova, K., Završnik, D., Saso, L., Durić, K., & Mladenka, P. (2018). 9-(4'-dimethylaminophenyl)-2,6,7-trihydroxy-xanthene-3-one is a Potentially Novel Antiplatelet Drug which Antagonizes the Effect of Thromboxane A2. *Medicinal Chemistry*, 14(2), 200-209. DOI: 10.2174/1573406413666171010102535
- Baroni, M., Costantino, G., Cruciani, G., Riganelli, D., Valigi, R., & Clementi, S. (1993). Generating optimal linear PLS estimations (GOLPE): an advanced chemometric tool for handling 3D- QSAR problems. *Quantitative Structure- Activity Relationships*, 12(1), 9-20. DOI: 10.1002/qsar.19930120103
- Castanheiro, R. A., Silva, A., Campos, N. A., Nascimento, M. S., & Pinto, M. M. (2009). Antitumor activity of some prenylated xanthenes. *Pharmaceuticals*, 2(2), 33-43. DOI: 10.3390/ph2020033
- Chem Axon. (2017). Marvin Sketch V17.27. Retrieved from <https://chemaxon.com/products/marvin>.
- Cambridge Soft Corporation (2015). ChemBio3D Ultra 13.0. Retrieved from <http://www.cambridgesoft.com>.
- Cambridge Soft Corporation (2002). ChemDraw—Chemical drawing software. Retrieved from <http://www.cambridgesoft.com>.
- Chibale, K., Visser, M., van Schalkwyk, D., Smith, P. J., Saravanamuthu, A., & Fairlamb, A. H. (2003). Exploring the potential of xanthene derivatives as trypanothione reductase inhibitors and chloroquine potentiating agents. *Tetrahedron*, 59(13), 2289-2296. DOI: 10.1016/S0040-4020(03)00240-0
- Cramer, R. D. (1993). Partial least squares (PLS): its strengths and limitations. *Perspectives in Drug Discovery and Design*, 1(2), 269-278. DOI: 10.1007/BF02174528
- Cramer, R. D., Patterson, D. E., & Bunce, J. D. (1988). Comparative molecular field analysis (CoMFA). 1. Effect of shape on binding of steroids to carrier proteins. *Journal of the American Chemical Society*, 110(18), 5959-5967. DOI: 10.1021/ja00226a005

Frisch, M. J., Trucks, G. W., Schlegel, H. B., Scuseria, G. E., Robb, M. A., Cheeseman, J. R., Scalmani, G., Barone, V., Mennucci, B., Petersson, G.A., & Nakatsuji, H. (2009). Gaussian 09 (Revision A. 02)[Computer software]. Gaussian Inc., Wallingford CT.

Gagić, Ž., Nikolić, K., Ivković, B., Filipić, S., & Agbaba, D. (2016). QSAR studies and design of new analogs of vitamin E with enhanced antiproliferative activity on MCF-7 breast cancer cells. *Journal of the Taiwan Institute of Chemical Engineers*, 59, 33-44. DOI: 10.1016/j.jtice.2015.07.019

Gazivoda, T., Raić-Malić, S., Krištafor, V., Makuc, D., Plavec, J., Bratulić, S., Kraljević-Pavelić, S., Pavelić, K., Naesens, L., Andrei, G., Snoeck, R., Balzarini, J., & Mintas, M. (2008). Synthesis, cytostatic and anti-HIV evaluations of the new unsaturated acyclic C-5 pyrimidine nucleoside analogues. *Bioorganic & medicinal chemistry*, 16(10), 5624-5634. DOI: 10.1016/j.bmc.2008.03.074

Giri, R., Goodell, J. R., Xing, C., Benoit, A., Kaur, H., Hiasa, H., & Ferguson, D. M. (2010). Synthesis and cancer cell cytotoxicity of substituted xanthenes. *Bioorganic & medicinal chemistry*, 18(4), 1456-1463. DOI: 10.1016/j.bmc.2010.01.018

Golbraikh, A., & Tropsha, A. (2002). Beware of q²!. *Journal of molecular graphics and modelling*, 20(4), 269-276. DOI: 10.1016/s1093-3263(01)00123-1

Jiang, D. J., Dai, Z., & Li, Y. J. (2004). Pharmacological effects of xanthenes as cardiovascular protective agents. *Cardiovascular Drug Reviews*, 22(2), 91-102. DOI: 10.1111/j.1527-3466.2004.tb00133.x

Kumar, D., Sharma, P., Singh, H., Nepali, K., Gupta, G. K., Jain, S. K., & Ntie-Kang, F. (2017). The value of pyrans as anticancer scaffolds in medicinal chemistry. *RSC advances*, 7(59), 36977-36999. DOI: 10.1039/C7RA05441F

Labute, P. (2000). A widely applicable set of descriptors. *Journal of Molecular Graphics and Modelling*, 18(4-5), 464-477. DOI: 10.1016/s1093-3263(00)00068-1

Liu, Y., Ke, Z., Cui, J., Chen, W. H., Ma, L., & Wang, B. (2008). Synthesis, inhibitory activities, and QSAR study of xanthone derivatives as α -glucosidase inhibitors. *Bioorganic & medicinal chemistry*, 16(15), 7185-7192. DOI: 10.1016/j.bmc.2008.06.043

Molecular Discovery Ltd. (2009). Pentacle, Version 1.0.7. Retrieved from <http://www.moldiscovery.com>.

Na, Y. (2009). Recent cancer drug development with xanthone structures. *Journal of Pharmacy and Pharmacology*, 61(6), 707-712. DOI: 10.1211/jpp/61.06.0002

Naya, A., Sagara, Y., Ohwaki, K., Saeki, T., Ichikawa, D., Iwasawa, Y., Noguchi, K., & Ohtake, N. (2001). Design, synthesis, and discovery of a novel CCR1 antagonist. *Journal of medicinal chemistry*, 44(9), 1429-1435. DOI: 10.1021/jm0004244

Núñez, M. B., Maguna, F. P., Okulik, N. B., & Castro, E. A. (2004). QSAR modeling of the MAO inhibitory activity of xanthenes derivatives. *Bioorganic & medicinal chemistry letters*, 14(22), 5611-5617. DOI: 10.1016/j.bmcl.2004.08.066

- Ojha, P. K., Mitra, I., Das, R. N., & Roy, K. (2011). Further exploring rm2 metrics for validation of QSPR models. *Chemometrics and Intelligent Laboratory Systems*, 107(1), 194-205. DOI: 10.1016/j.chemolab.2011.03.011
- Omolo, J. J., Johnson, M. M., Van Vuuren, S. F., & De Koning, C. B. (2011). The synthesis of xanthenes, xanthenediones, and spirobenzofurans: their antibacterial and antifungal activity. *Bioorganic & medicinal chemistry letters*, 21(23), 7085-7088. DOI: 10.1016/j.bmcl.2011.09.088
- Ornstein, P. L., Arnold, M. B., Bieisch, T. J., Wright, R. A., Wheeler, W. J., & Schoepp, D. D. (1998). [3H] LY341495, a highly potent, selective and novel radioligand for labeling group II metabotropic glutamate receptors. *Bioorganic & medicinal chemistry letters*, 8(14), 1919-1922. DOI: 10.1016/s0960-894x(98)00329-1
- Pedro, M., Cerqueira, F., Sousa, M. E., Nascimento, M. S. J., & Pinto, M. (2002). Xanthenes as inhibitors of growth of human cancer cell lines and their effects on the proliferation of human lymphocytes in vitro. *Bioorganic & medicinal chemistry*, 10(12), 3725-3730. DOI: 10.1016/s0968-0896(02)00379-6
- Pinto, M. M. M., Sousa, M. E., & Nascimento, M. S. J. (2005). Xanthone derivatives: new insights in biological activities. *Current medicinal chemistry*, 12(21), 2517-2538. DOI: 10.2174/092986705774370691
- Recanatini, M., Bisi, A., Cavalli, A., Belluti, F., Gobbi, S., Rampa, A., Valenti, P., Palzer, M., Paluszczak, A., & Hartmann, R. W. (2001). A new class of nonsteroidal aromatase inhibitors: design and synthesis of chromone and xanthone derivatives and inhibition of the P450 enzymes aromatase and 17 α -hydroxylase/C17, 20-lyase. *Journal of medicinal chemistry*, 44(5), 672-680. DOI: 10.1021/jm000955s
- Roothaan, C. C. J. (1951). New developments in molecular orbital theory. *Reviews of modern physics*, 23(2), 69. DOI: 10.1103/RevModPhys.23.69
- Santos, C. M., Freitas, M., & Fernandes, E. (2018). A comprehensive review on xanthone derivatives as α -glucosidase inhibitors. *European journal of medicinal chemistry*, 157, 1460-1479. DOI: 10.1016/j.ejmech.2018.07.073
- Santos, C. M., Freitas, M., Ribeiro, D., Gomes, A., Silva, A. M., Cavaleiro, J. A., & Fernandes, E. (2010). 2,3-Diarylxanthenes as strong scavengers of reactive oxygen and nitrogen species: a structure-activity relationship study. *Bioorganic & medicinal chemistry*, 18(18), 6776-6784. DOI: 10.1016/j.bmc.2010.07.044
- Sharma, B. K., Sarbhai, K., & Singh, P. (2010). A rationale for the activity profile of arylpiperazinylthioalkyls as 5-HT_{1A}-serotonin and α 1-adrenergic receptor ligands. *European journal of medicinal chemistry*, 45(5), 1927-1934. DOI: 10.1016/j.ejmech.2010.01.034
- Simulations Plus, Inc. (2013). ADMET Predictor v. 9.0. Retrieved from <http://www.simulations-plus.com/>.
- Software Tools. (n.d.). *DTC Lab*. <http://dtclab.webs.com/software-tools>.
- Stewart, J. J. (1989a). Optimization of parameters for semiempirical methods I. Method. *Journal of computational chemistry*, 10(2), 209-220. DOI: 10.1002/jcc.540100208

Stewart, J. J. (1989b). Optimization of parameters for semiempirical methods II. Applications. *Journal of computational chemistry*, 10(2), 221-264. DOI: 10.1002/jcc.540100209

Talete srl. (2010). Dragon 6. Retrieved from <http://www.talete.mi.it/>.

Thanikaivelan, P., Subramanian, V., Rao, J. R., & Nair, B. U. (2000). Application of quantum chemical descriptor in quantitative structure activity and structure property relationship. *Chemical Physics Letters*, 323(1-2), 59-70. DOI: 10.1016/S0009-2614(00)00488-7

Todeschini, R., & Consonni, V. (2009). *Molecular descriptors for chemoinformatics* (2nd ed.). Weinheim, Germany: Wiley-VCH.

Tropsha, A. (2010). Best practices for QSAR model development, validation, and exploitation. *Molecular informatics*, 29(6- 7), 476-488. DOI: 10.1002/minf.201000061

Umetrics AB. (2015). SIMCA Program Version 14.1. Retrieved from www.umetrics.com.

Veljović, E., Špirtović-Halilović, S., Muratović, S., Osmanović, A., Badnjević, A., Gurbeta, L., Tatlić, B., Zorlak, Z., Imamović, S., Husić, Đ., Završnik, D. (2017). Artificial neural network and docking study in design and synthesis of xanthenes as antimicrobial agents. In *CMBEIH 2017* (pp. 617-626). Springer, Singapore. DOI: 10.1007/978-981-10-4166-2_93

Veljović, E., Špirtović-Halilović, S., Muratović, S., Osmanović, A., Haverić, S., Haverić, A., Hadžić, M., Salihović, M., Malenica, M., Šapčanin, A., & Završnik, D. (2019). Antiproliferative and genotoxic potential of xanthen-3-one derivatives. *Acta Pharmaceutica*, 69(4), 683-694. DOI: 10.2478/acph-2019-0044

Veljović, E., Špirtović-Halilović, S., Muratović, S., Osmanović, A., Novaković, I., Trifunović, S., & Završnik, D. (2018). Synthesis and biological evaluation of xanthen-1, 8-dione derivatives. *Bulletin of the Chemists and Technologists of Bosnia and Herzegovina*, 51, 13-18.

Veljović, E., Špirtović-Halilović, S., Muratović, S., Valek Žulj, L., Roca, S., Trifunović, S., Osmanović, A., & Završnik, D. (2015). 9-aryl substituted hydroxylated xanthen-3-ones: synthesis, structure and antioxidant potency evaluation. *Croatica Chemica Acta*, 88(2), 121-127. DOI: 10.5562/cca2595

Wang, X. Z., Jia, Z., Yang, H. H., & Liu, Y. J. (2018). Dibenzoxanthenes induce apoptosis and autophagy in HeLa cells by modeling the PI3K/Akt pathway. *Journal of Photochemistry and Photobiology B: Biology*, 187, 76-88. DOI: 10.1016/j.jphotobiol.2018.08.001

Winter, R. W., Ignatushchenko, M., Ogundahunsi, O. A., Cornell, K. A., Oduola, A. M., Hinrichs, D. J., & Riscoe, M. K. (1997). Potentiation of an antimalarial oxidant drug. *Antimicrobial agents and chemotherapy*, 41(7), 1449-1454.

Wold, S., Eriksson, L., & Clementi, S. (1995). Statistical validation of QSAR results. In H. Van de Waterbeemd (Ed.), *Chemometric methods in molecular design* (pp. 309-338). Weinheim, Germany: VCH. DOI: 10.1002/9783527615452.ch5

Wold, S., Sjöström, M., & Eriksson, L. (2001). PLS-regression: a basic tool of chemometrics. *Chemometrics and intelligent laboratory systems*, 58(2), 109-130. DOI: 10.1016/S0169-7439(01)00155-1

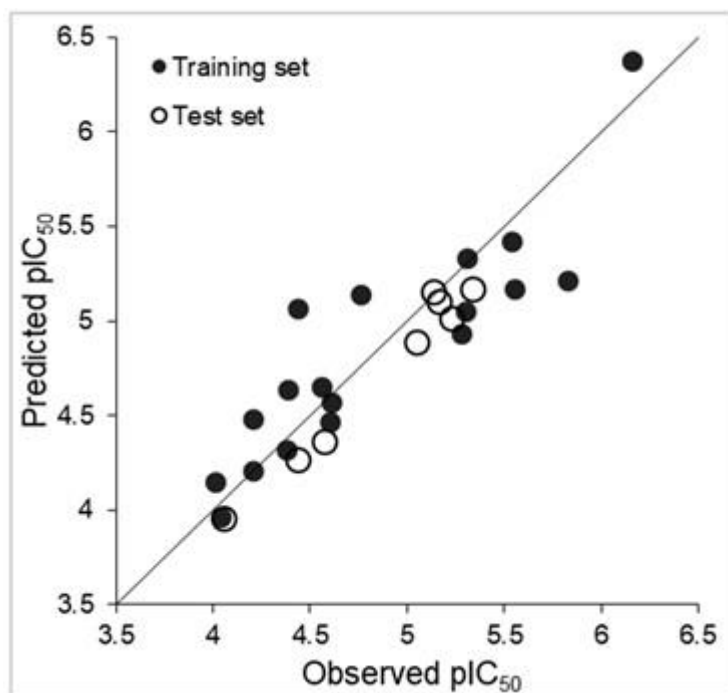
Woo, S., Jung, J., Lee, C., Kwon, Y., & Na, Y. (2007). Synthesis of new xanthone analogues and their biological activity test—Cytotoxicity, topoisomerase II inhibition, and DNA cross-linking study. *Bioorganic & medicinal chemistry letters*, 17(5), 1163-1166. DOI: 10.1016/j.bmcl.2006.12.030

Yen, C. T., Nakagawa-Goto, K., Hwang, T. L., Morris-Natschke, S. L., Bastow, K. F., Wu, Y. C., & Lee, K. H. (2012). Design and synthesis of gambogic acid analogs as potent cytotoxic and anti-inflammatory agents. *Bioorganic & medicinal chemistry letters*, 22(12), 4018-4022. DOI: 10.1016/j.bmcl.2012.04.084

Zukić, S., Veljović, E., Špirtović-Halilović, S., Muratović, S., Osmanović, A., Trifunović, S., Novaković, I., & Završnik, D. (2018). Antioxidant, Antimicrobial and Antiproliferative Activities of Synthesized 2,2,5,5-Tetramethyl-9-aryl-3,4,5,6,7,9-hexahydro-1H-xanthene-1,8(2H)-dione Derivatives. *Croatica Chemica Acta*, 91(1), 1-10. DOI: 10.5562/cca3225

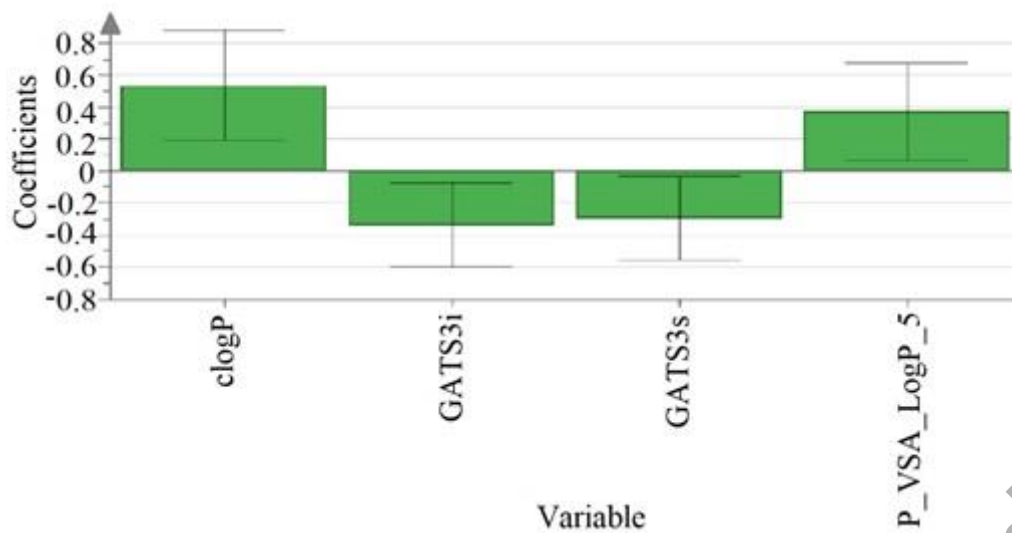
Accepted Manuscript

Fig. 1. Scatter plot of observed vs predicted pIC_{50} for 2D-QSAR model



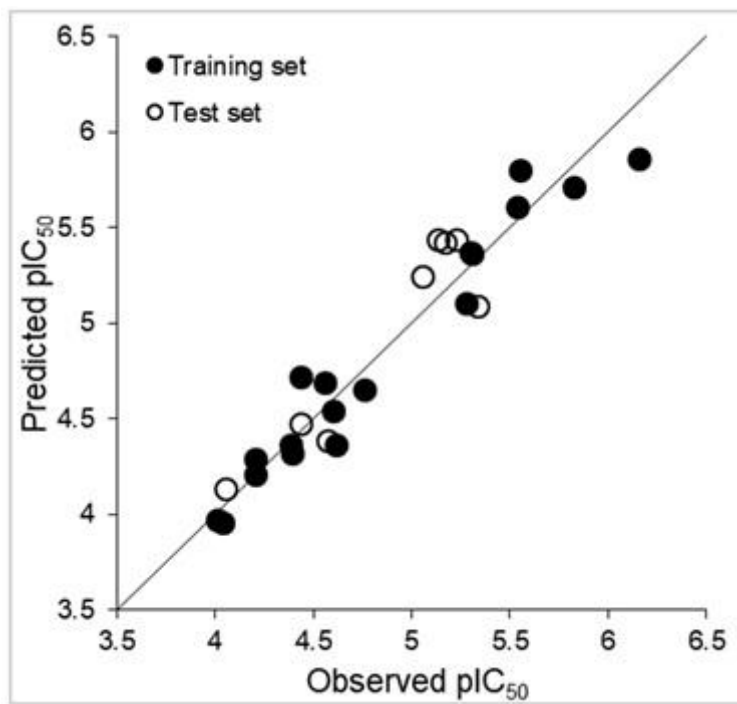
Accepted Manuscript

Fig. 2. The coefficient plot of most important descriptors for 2D-QSAR model



Accepted Manuscript

Fig. 3. Scatter plot of observed vs predicted pIC_{50} for 3D-QSAR model



Accepted Manuscript

Fig. 4. Coefficients of PLS regression for the most important GRIND descriptors with positive and negative descriptors values for 3D-QSAR model

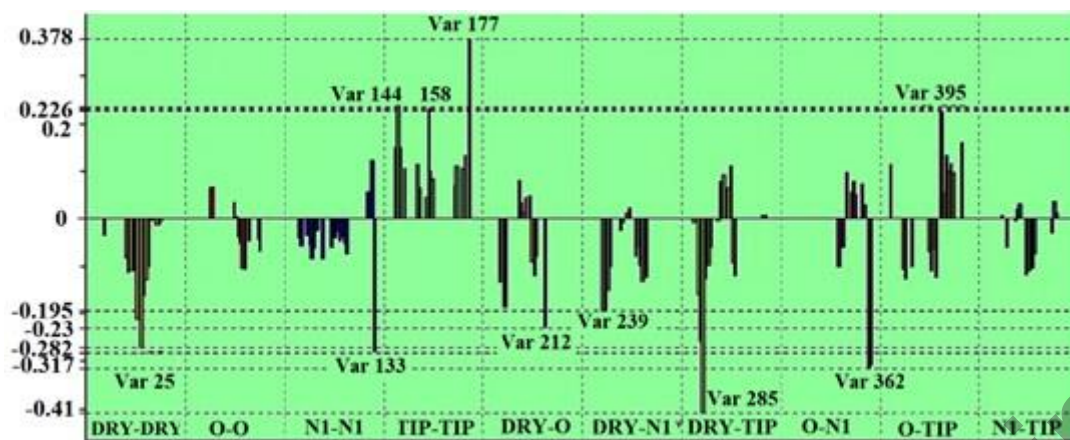
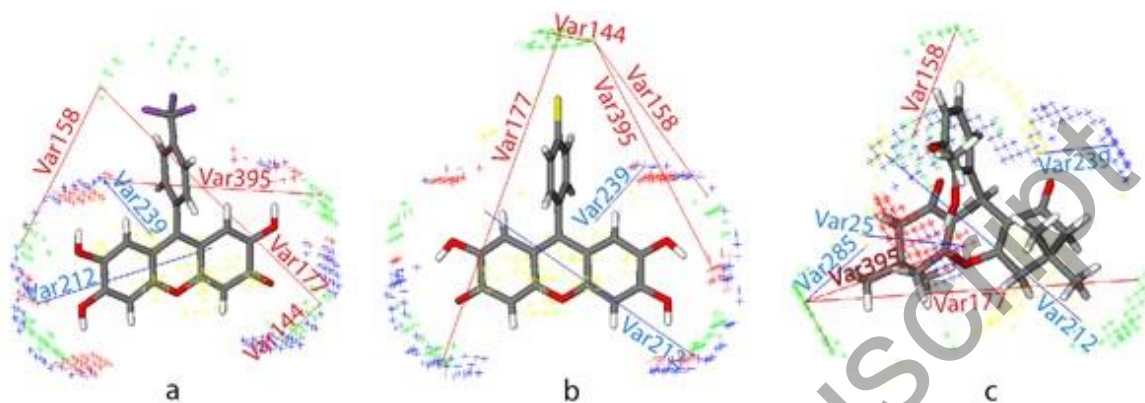
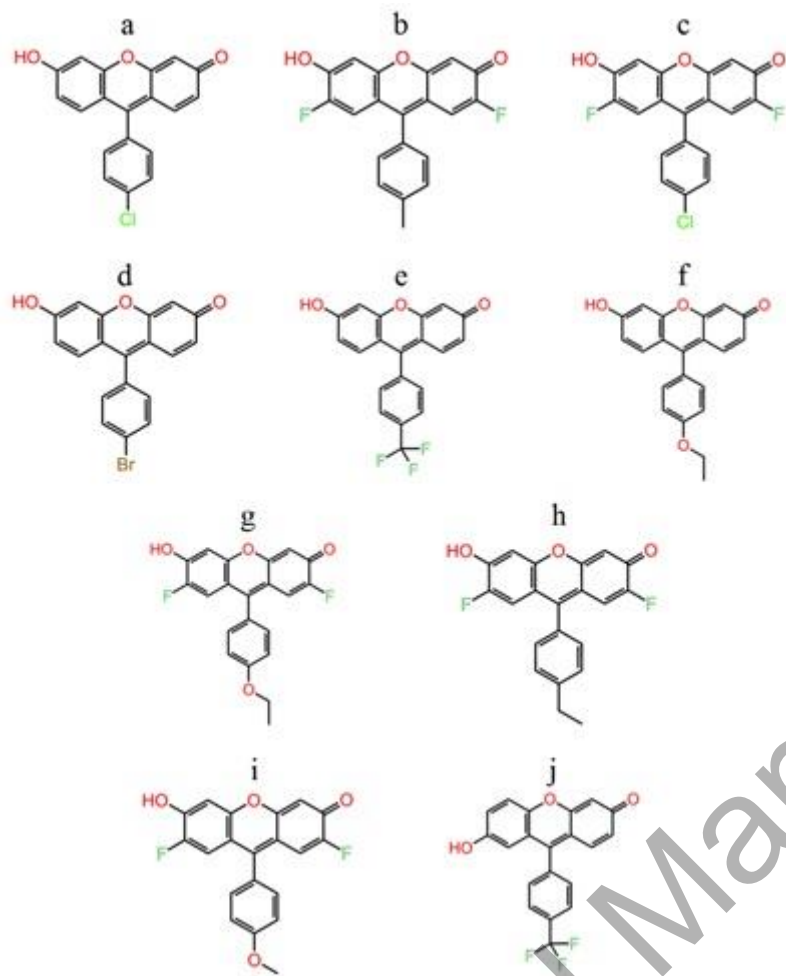


Fig. 5. 3D-QSAR pharmacophore model for a) compound **9**, b) compound **14**, and c) compound **4-II**. The hydrophobic regions (DRY) are presented in yellow, steric hot spots (TIP) in green, H-bond donor regions (O) in pink and H-bond acceptor regions (N1) are presented in blue. Distances in red are favorable while distances in blue are not favorable for antiproliferative activity.



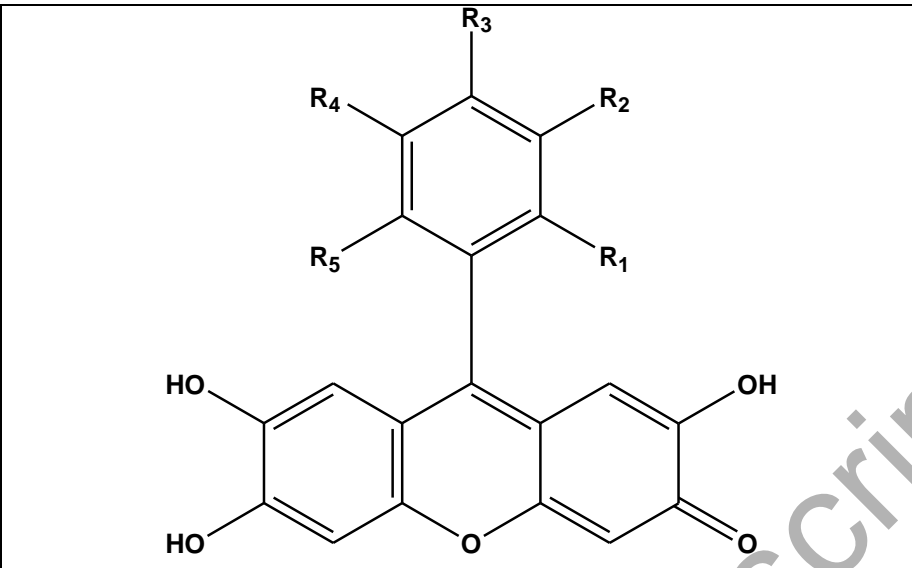
Accepted Manuscript

Fig. 6. New designed compounds of xanthene derivatives



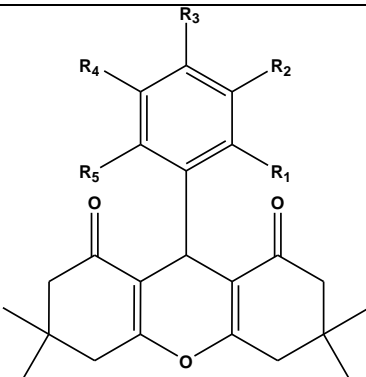
Accepted Manuscript

Table 1. Chemical structures of 9-aryl substituted 2,6,7-trihydroxyxanthen-3-one derivatives and their antiproliferative activity on HeLa cell lines



Compounds	R ₁	R ₂	R ₃	R ₄	R ₅	IC ₅₀ [μM]
1	OH	H	H	Br	H	5.3
2	OH	OCH ₃	H	H	H	8.9
3	H	OH	OH	H	H	27.5
4	H	OCH ₃	OCH ₃	H	H	4.9
5	H	OCH ₃	OH	OCH ₃	H	>100
6	H	OCH ₃	OH	NO ₂	H	36.6
7	H	H	OC ₂ H ₅	H	H	2.9
8	H	H	N(CH ₃) ₂	H	H	5
9	H	H	CF ₃	H	H	0.7
10	H	H	NHCOCH ₃	H	H	40.8
11	H	Br	H	H	H	1.5
12	Cl	H	H	H	F	4.6
13	Cl	H	H	H	H	17.3
14	H	H	Cl	H	H	2.8
15	H	H	F	H	H	6.8
16	OCH ₃	H	H	H	H	36.7
17	H	Cl	H	H	H	7.3
18	OH	H	H	NO ₂	H	91.5
19	H	H	H	H	H	5.9
20	H	H	NO ₂	H	H	41.5

Table 2. Chemical structures of 3,3,6,6,-tetramethyl-9-aryl-substituted-xanthen-1,8(2H)-dione derivatives and their antiproliferative activity on HeLa cell lines



Compounds	R ₁	R ₂	R ₃	R ₄	R ₅	IC ₅₀ [μM]
1-II	H	H	H	H	H	>100
2-II	OH	OH	H	H	H	>100
3-II	H	OH	OH	H	H	87.9
4-II	OH	OCH ₃	H	H	H	97.9
5-II	NO ₂	H	H	H	H	>100
6-II	H	H	NO ₂	H	H	>100
7-II	OH	H	H	NO ₂	H	>100
8-II	F	H	H	H	H	>100
9-II	H	F	H	H	H	>100
10-II	H	H	F	H	H	>100
11-II	H	H	CF ₃	H	H	>100
12-II	H	Cl	H	H	H	>100
13-II	H	H	Cl	H	H	>100
14-II	Br	H	CH ₃	H	H	5.6
15-II	H	H	Br	H	H	>100
16-II	H	Br	H	Br	H	62.4
17-II	H	H	NHCOCH ₃	H	H	>100
18-II	OH	H	H	Br	H	62.2
19-II	H	H	N(CH ₃) ₂	H	H	>100
20-II	OCH ₃	OCH ₃	H	Br	H	24.4
21-II	H	OCH ₃	OCH ₃	H	H	>100
22-II	OCH ₃	H	OCH ₃	H	OCH ₃	25.2
23-II	H	OCH ₃	OH	NO ₂	H	>100
24-II	OCH ₃	H	H	OCH ₃	H	26.9
25-II	H	OCH ₃	OH	OCH ₃	H	>100

Table 3. Experimentally obtained IC₅₀ values

IC ₅₀ values (μM)		
Compounds	HeLa cell lines	BJ
13	17.3	9.1
14	2.8	6.4
15	6.8	21.9
16	36.7	7
17	7.3	28.4
18	91.5	79
19	5.9	6.6
20	41.5	8.8

Table 4. Calculated statistical parameters of 2D-QSAR and 3D-QSAR models

Model	Q ²	R ²	RMSEE	RMSEP	F	p	rpred ²	rm ²	reverse rm ²	average rm ²	delta rm ²
2D	0.741	0.792	0.289	0.152	10.756	5E-04	0.875	0.899	0.93	0.915	0.03
3D	0.830	0.950	0.147	0.207	/	/	0.769	0.674	0.814	0.744	0.139

Table 5. Most important favorable and unfavorable GRIND variables in the 3D-QSAR model

Variable	Pair of probes	Distance [Å]	Comments on GRIND variable
144 (positive)	TIP-TIP	2.4-2.8	Represents two steric hot spots at a smaller distance described by v158. Present in all molecular structures except 4-II.
158 (positive)	TIP-TIP	8-8.4	Two steric hot spots at the optimal distance between C'-4 position of the phenyl ring and xanthene heterocycle. Present in all compounds.
177 (positive)	TIP-TIP	15.6-16	Represent distance between two steric hot spots. Not presented in compounds 1, 3, 13, 16, and 18 .
25 (negative)	DRY-DRY	10-10.4	Represent distance between two hydrophobic regions. Present in the least active molecular structures. Not presented in compounds 3, 4, 9, 11, 13, and 14 .
133 (negative)	N1-N1	16.4-16.8	Represent distance between two H-bond acceptor groups. Present only in molecules 10 and 20 .
239 (negative)	DRY-N1	3.6-4	Distance between the hydrophobic region of the phenyl ring and H-bond acceptor group in the xanthene nucleus. Present in all most active and least active molecular structures except in 18-II and 22-II .
362 (negative)	O-N1	16-16.4	Distance between H-bond donor and H-bond acceptor. Present only in compounds 10 and 20 .
285 (negative)	DRY-TIP	3.6-4	Distance between the hydrophobic region and steric hot spot. Present in all least active molecular structures. Not presented in active compounds 8, 9, 11, and 14 .
212 (negative)	DRY-O	11.2-11.6	Distance between the hydrophobic region and H-bond donor group OH of the xanthene nucleus. Present in all molecular structures except in 16-II and 18-II .
395 (positive)	O-TIP	10.8-11.2	Distance between H-bond donor and steric hot spot region on the phenyl ring or xanthene nucleus. Present in all molecular structures.

Table 6. ADMET properties and pIC₅₀ of the examined data set

<i>ADMET properties of data set and pIC₅₀ values of examined compounds</i>								
Molecule	ADMET_Risk	MlogP	RuleOf5	CYP_Risk	hERG_Filter	TOX_Risk	MWt	exp. pIC ₅₀
1	1.163	1.609	0	0	No (96%)	0.877	415.204	5.276
2	0.245	0.738	0	0.235	No (96%)	0.000	366.329	5.051
3	2.851	0.510	0	0.526	No (96%)	0.000	352.302	4.56
4	1.658	0.961	0	0.295	No (96%)	1.362	380.356	5.31
6	4.745	0.618	0	0.619	No (96%)	2.000	411.327	4.436
7	1.404	1.720	0	0.404	No (96%)	1.000	364.357	5.538
8	0.020	1.720	0	0.02	No (96%)	0.000	363.372	5.301
9	2.000	2.602	0	1	No (96%)	1.000	388.302	6.155
10	0.584	1.297	0	0.584	No (96%)	0.000	377.356	4.389
11	0.957	2.381	0	0	No (96%)	0.957	399.205	5.824
12	2.633	2.381	0	0.633	No (96%)	2.000	372.739	5.337
13	0.414	2.269	0	0	No (87%)	0.000	354.749	4.762
14	0.025	2.269	0	0	No (87%)	0.000	354.749	5.553
15	1.230	2.156	0	0.356	No (96%)	0.874	338.294	5.167
16	0.000	1.497	0	0	No (96%)	0.000	350.33	4.435
17	0.182	2.269	0	0	No (87%)	0.182	354.749	5.137
18	4.000	1.121	0	0	No (96%)	2	381.3	4.038
19	0.000	2.041	0	0	No (96%)	0.000	320.304	5.229
20	2.478	1.860	0	0	No (96%)	2	365.301	4.382
3-II	2.266	2.760	0	0.157	No (96%)	0.967	382.46	4.056
4-II	4.331	2.971	0	0.891	No (87%)	0.554	396.487	4.009
16-II	7.463	4.468	2	1.892	No (87%)	1.000	508.263	4.205
18-II	5.027	3.352	0	0.567	No (81%)	0.877	445.361	4.206
20-II	6.383	3.241	0	1	No (87%)	1.000	489.415	4.613
22-II	5.783	2.368	0	1	No (96%)	0.942	440.54	4.599
24-II	4.528	2.668	0	1.025	No (96%)	0.000	410.514	4.57

MWt: molecular weight; MlogP: Moriguchi estimation of log P; RuleOf5: Lipinski's rule of 5, a score indicating the number of potential problems a compound is expected to have with passive oral absorption; CYP_Risk: risk connected with P450 oxidation, a score in the 0-8 range indicating the number of potential problems a compound might have due to metabolism by or inhibition of five major cytochrome P450s; hERG Filter: qualitative estimation of the affinity to the hERG potassium channel in human; TOX_Risk: risk connected with predicted toxicity, a score in 0-6 range indicating the number of potential toxicity problems a compound might have; ADMET risk: a score in the 0-24 range indicating the number of potential ADMET problems a compound might have

Table 7. ADMET properties and predicted pIC₅₀ of new designed compounds

<i>ADMET properties of new designed molecules and their predicted pIC₅₀ values</i>								
	ADMET_Risk	MlogP	RuleOf5	CYP_Risk	hERG_Filter	TOX_Risk	MWt	pred. pIC ₅₀
a	2.095	3.085	0	0	Yes (65%)	0.798	322.75	6.525
b	2.011	3.576	0	0.011	No (87%)	1	338.313	6.483
c	3	3.576	0	0	No (56%)	2	358.731	6.412
d	2.443	3.197	0	0	Yes (59%)	1	367.206	6.353
e	3.618	3.418	0	1.295	Yes (57%)	1	356.303	6.321
f	2.715	2.501	0	0.001	No (61%)	1.745	332.358	6.267
g	2.373	2.987	0	0.634	No (96%)	1	368.339	6.214
h	2.5	3.795	0	0.341	No (81%)	1	352.34	6.156
i	1.668	2.769	0	0.426	No (96%)	1	354.312	6.146
j	3.301	3.418	0	0.807	No (47%)	1	356.303	6.137

MWt: molecular weight; MlogP: Moriguchi estimation of log P; RuleOf5: Lipinski's rule of 5, a score indicating the number of potential problems a compound is expected to have with passive oral absorption; CYP_Risk: risk connected with P450 oxidation, a score in the 0-8 range indicating the number of potential problems a compound might have due to metabolism by or inhibition of five major cytochrome P450s; hERG Filter: qualitative estimation of the affinity to the hERG potassium channel in human; TOX_Risk: risk connected with predicted toxicity, a score in 0-6 range indicating the number of potential toxicity problems a compound might have; ADMET risk: a score in the 0-24 range indicating the number of potential ADMET problems a compound might have